Enhancing the RIM process with pulsation technology: CFD study
Proceedings of European Congress of Chemical Engineering (ECCE-6)
Copenhagen, 16-20 September 2007

Enhancing the RIM process with pulsation technology: CFD study

E.Erkoç,[a] R.J.Santos,[a] M.M.Dias,[a] J.C.B.Lopes[a,b]

[a]*Laboratory of Separation and Reaction Engineering, Department of Chemical Engineering, Faculdade de Engenharia da Universidade do Porto,Rua Dr. Roberto Frias 4200-465 Porto, Portugal*
[b]*Fluidinova-Engenharia de Fluidos, SA, Tecmaia, Rua Engº Frederico Ulrich, 2650, 4470-605, Moreira da Maia, Portugal*

Abstract

Numerical simulations were performed to study the effect of pulsation on the flow dynamics of a 2D laminar T-jets mixer. Different strategies, frequencies and amplitudes of the opposed jets pulsation were tested, aiming to assess its effect on the mixing dynamics of the flow field. The pulsation frequencies were set in relation to the natural oscillation frequencies of the flow field. It is found that out phase pulsation of the opposed jets with frequency close to the jets natural oscillations frequencies, ϕ, enhance the order of the system resulting in a flow field with a well defined repetitive generation of vortices. Imposing pulsations to the system that have different frequency values from the non-forced flow dynamics enhance its disorder. The study showed that the amplitude of the oscillation has a strong effect on the flow field, and that this effect increases with increasing amplitude up to the extreme case where the imposed pulsation completely drives the dynamics of the system.

Keywords: RIM, Chaotic Mixing, T-Jets, Oscillation and Pulsation

Introduction

Reaction Injection Moulding (RIM) is a process where two monomer streams, generally polyol and isocyanate are contacted in a T-jets mixer, the mixing chamber, at high velocities, up to 100m/s, but at low jets Reynolds number, $100<Re<600$, due to the viscosity of monomers that ranges from 20 to 1000 mPa.s (Macosko, 1989). Figure 1 shows the geometry of a typical RIM machine mixing chamber.

Previous works by the present authors research team have extensively studied mixing mechanisms in RIM (Santos *et al.*, 2002, Teixeira *et al.*, 2005, and Santos *et al.*, 2005) and the mechanisms of jets natural oscillations and its control (Xiaojin *et al.*, 2007 and Erkoç *et al.*, 2007). Other RIM mixing studies of relevance were carried out by Lee *et al.* (1980), Tucker and Suh (1980), Kolodziej *et al.* (1982 and 1986),

Sandell *et al.* (1985), Kush *et al.* (1989), Wood *et al.* (1991), Johnson *et al.* (1996), Johnson and Wood (2000) and Trautmann and Piesche, (2001). From all the available literature on mixing in RIM, the pulsation of the jets was only tackled in Bierdel and Piesche (2001) that analysed the influence of pulsation amplitude on the quality of mixing. Other authors used pulsation techniques on T-jets and Y-jets mixers to perturb the flow field and cause the onset of convective mixing (Deshmukh *et al.*, 2000 and 2001, Zhongliang *et al.*, 2002, and Ito and Komori, 2006), a technique usually referred as active mixing.

In the case of this study, mixing is not engaged from the pulsation, since the flow field in the mixing chamber at the Reynolds number value of 300 here studied has natural advective chaotic patterns. The purpose here is to scrutinise the interaction between the flow natural oscillations and the imposed jets oscillations, namely its effect on the flow dynamics and on the shape and evolution of the natural advective chaotic patterns formed downstream the opposed jets impingement point.
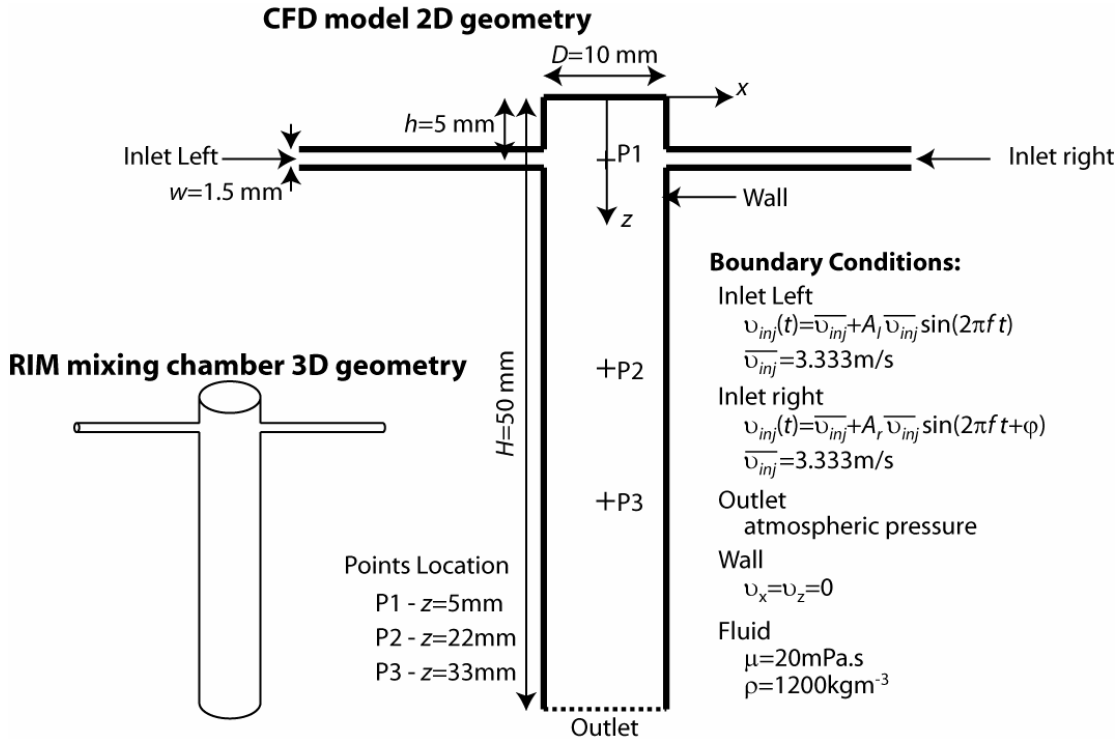
Figure 1 RIM machine typical mixing chamber geometry and its 2D representation and respective hydrodynamic model here used for the CFD simulations.

CFD Model

The flow field was simulated with Fluent[TM] using a 2D model of the mixing chamber shown in Figure 1 and previously described in Erkoç *et al.* (2007). The 2D chamber is rectangular, having 50 mm length and 10 mm width, connected to 20 mm long injectors whose centre is located at 5 mm from the close top of the chamber. The injectors averaged Reynolds number, Re, is defined for the 2D geometry as

$$Re = \rho \overline{v_{inj}} w / \mu \qquad \text{eq. 1}$$

where w is the injector width, which is 1.5 mm, μ is the viscosity that here is 20 mPa.s, ρ is the density that here is 1200 kg/m^3 and $\overline{v_{inj}}$ =3.333 m/s is the time and space average fluid velocity at the injectors. The boundary conditions were set as no slip in the walls, and the liquid leaves the chamber from a pressure outlet set at atmospheric conditions. The dynamic simulations were always started from a steady state solution of the flow field for Re =300. The pulsation of the jets is performed according to the following equations:

on the left injector $\qquad v_{inj}(t)_l = \overline{v_{inj}} + A_l \overline{v_{inj}} \sin(2\pi f t) \qquad$ eq. 2

on the right injector $\qquad v_{inj}(t)_r = \overline{v_{inj}} + A_r \overline{v_{inj}} \sin(2\pi f t + \varphi) \qquad$ eq. 3

where A_l and A_r are the left and right pulsation amplitudes, respectively, f the pulsation frequency and φ the phase displacement between right and left injector pulsation.

Results

The jets impingement point oscillates with a frequency ϕ around 200 Hz for the used fluid in the defined 2D geometry at Re =300. The tested pulsation frequencies are $f = \phi/2$=100 Hz, $f = \phi$=200 Hz, and $f = 2\phi$=400 Hz. The simulated cases are all at Re =300 and summarized in Table 1.

Table 1 Summary of simulated cases

Case Number	Pulsation Strategy	Amplitude and Frequency
1	No Pulsation	$A = 0$
2	Only one jet is pulsed	$A_l = 0.50$, $f = \phi$
3	On-Phase	$A_l = A_r = 0.50$, $f = \phi$, $\varphi = 0$
4	Out-of-Phase	$A_l = A_r = 0.25$, $f = \phi$, $\varphi = \pi\phi$
5	Out-of-Phase	$A_l = A_r = 0.50$, $f = \phi$, $\varphi = \pi\phi$
6	Out-of-Phase	$A_l = A_r = 1.00$, $f = \phi$, $\varphi = \pi\phi$
7	Out-of-Phase	$A_l = A_r = 0.50$, $f = 2\phi$, $\varphi = 2\pi\phi$
8	Out-of-Phase	$A_l = A_r = 0.50$, $f = \phi/2$, $\varphi = \pi\phi/2$

All simulations were performed dynamically using a fixed time step of 10^{-4} s. For each time step, the x component velocity, v_x, was recorded in the axis of the chamber at the following distances from the top: z=5 mm (at the impingement point, P1); z=22 mm (P2); and z=33 mm (P3). The simulations were started from parallel steady solution for Re =300, and ran for a period of 2 seconds of operation. The data from the first 300 milliseconds of the operation was eliminated, and the power spectra were obtained from the data of the remaining 1.7 s.

Figure 2 shows the streamlines at some selected time instants of the dynamic simulations of the eight defined cases. The same flow behaviour previously reported in Santos *et al.* (2002 and 2005) of the formation of a vortex street downstream the jets impingement point is observed for the eight cases. Some differences are yet observable between the flow fields:

- The vortices in Cases 2 and 3, corresponding to one side oscillation and on-phase oscillation, are more distorted, less rounded, than the case of no pulsation.
- The cases with out-of-phase pulsation present greater regularity of the vortex streak, namely Cases 4, 5, 6 and 8, except for Case 7, where pulsation frequency is 2ϕ.

Case 1   Case 2

Case 3   Case 4

Case 5   Case 6

Case 7   Case 8
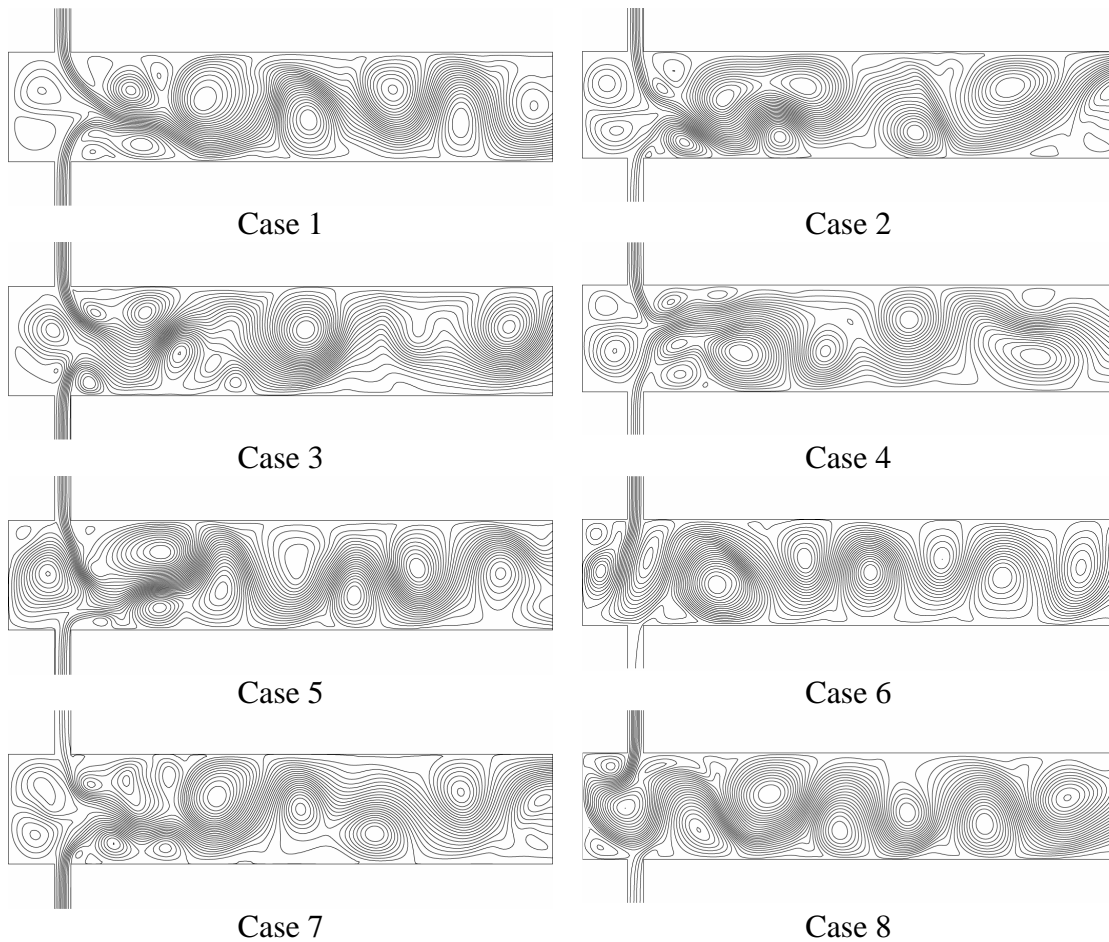
Figure 2 Streamlines of flow field in the mixing chamber from the dynamic simulations at average Re=300, using different pulsation strategies.

For a clear image of the pulsation effect on flow dynamics, the simulations time histories and its power spectra are presented. Figure 3 shows the time history of the *x* component of the dimensionless velocity $v_x^* = v_x / v_{inj}$ at the impingement point, P1, for the eight simulated cases, and Figure 4 shows the power spectra obtained from the

Case 1

Case 2

Case 3

Case 4

Case 5

Case 6

Case 7

Case 8
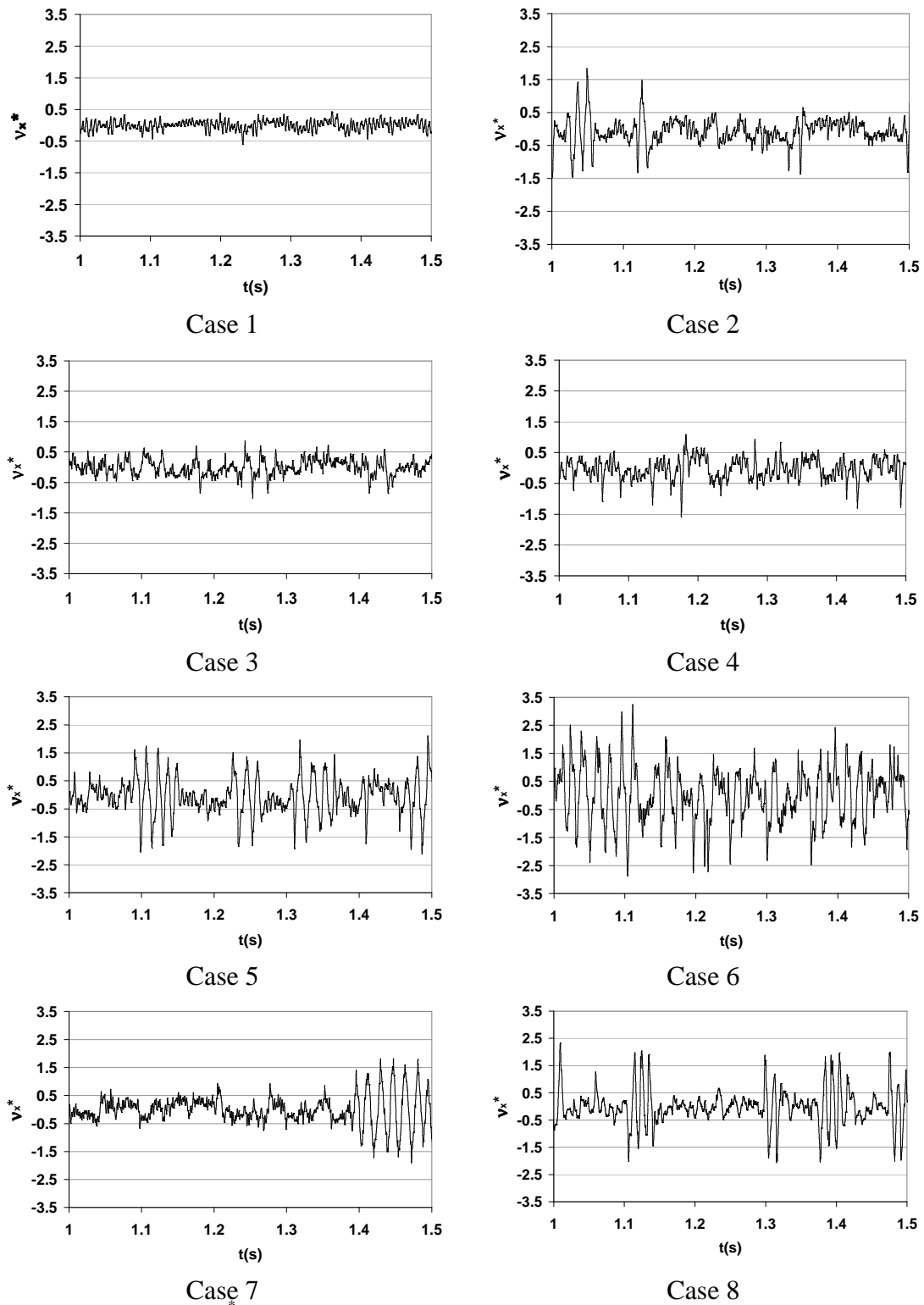
Figure 3 Time histories of v_x^* at the impingement point.

Case 1

Case 2

Case 3

Case 4

Case 5

Case 6

Case 7

Case 8
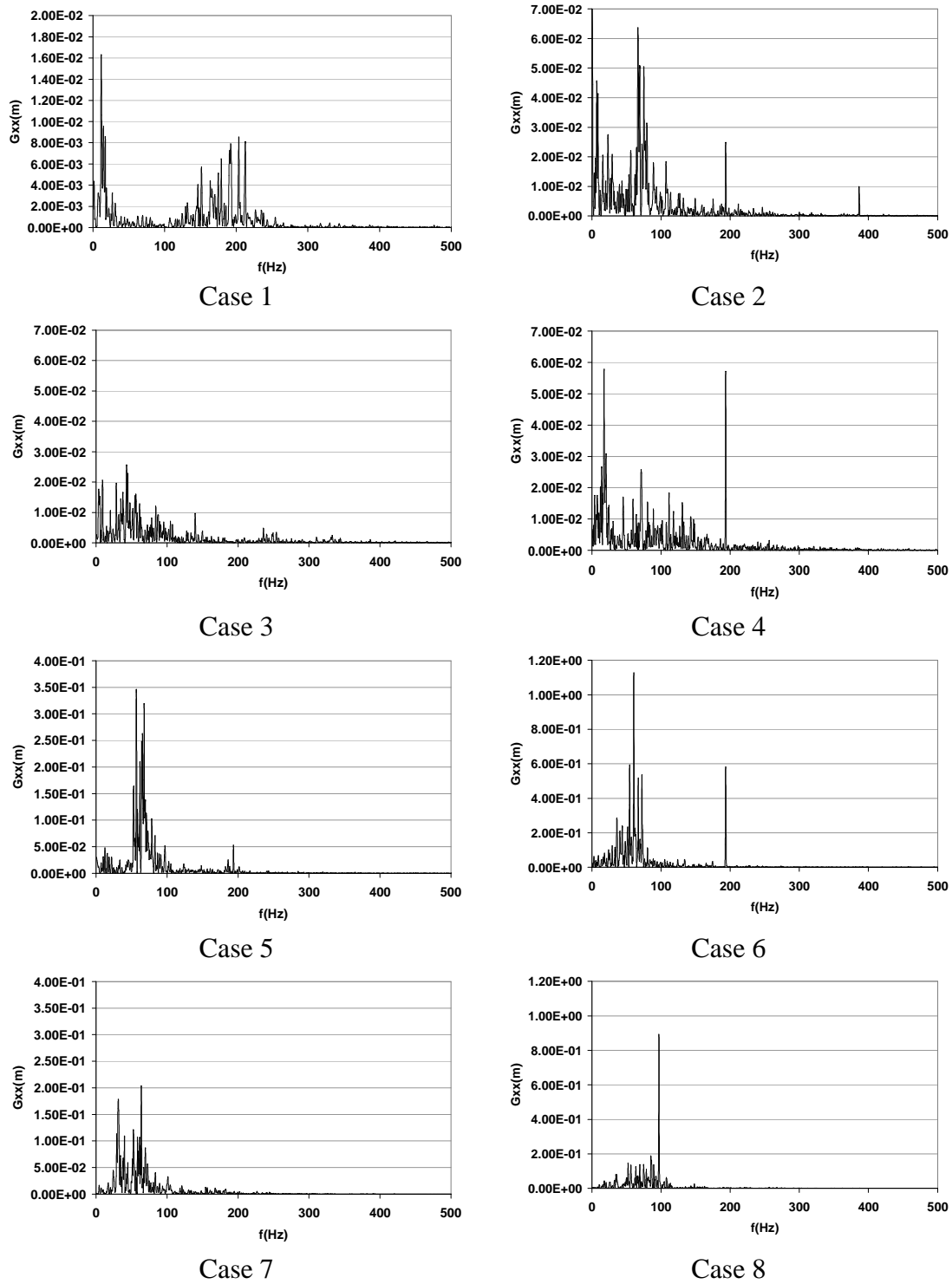
Figure 4 Power spectra at the impingement point from the dynamic simulations at average Re=300 using different pulsation strategies.

Table -2 Maximum energy levels from the power spectra of υ_x around f=200Hz, at the impingement point

Case Number	Max Energy, m
1	0.00843
2	0.0247
3	0.00168
4	0.0571
5	0.0530
6	0.583
7	0.000921
8	0.894 *

* taken at 100Hz

FFT of these time histories. The highest spectral energy values around the typical oscillation frequency of 200Hz are presented in Table 2.

For Case 1, where there is no pulsation imposed to the system, from the power spectra, a general great spread of energy around the jets typical frequency of oscillations, ϕ=200Hz is observed. The amplitude of the jets oscillations is also much less than for the cases of forced pulsation, as can be seen from the time histories of Figure 2 and Table 2, where the maximum energy value around the 200Hz frequency is seen to be almost one order of magnitude less than from the out-of-phase pulsation cases with $f = \phi$.

As one of the jets is pulsed, the appearance of a lower frequency peak, between 50 and 100Hz, is observed, as can be seen in Figure 2 and Table 2 for Case 2, which will be later identified on the analysis of downstream points, z=22 and 33 mm, by the passage of fully developed vortices.

The on-phase pulsation, Case 3, presents the lowest energy peaks, since both jets are pulsated simultaneously, their strengths keep balanced and there is no significant disturbance of the jets oscillation. When a jet loses its strength, it is not compensated by the opposed jet, which is also retracted, and when a jet increases its strength, it will not be able to push the other jet as its strength is matched-up by the opposed jet. The decrease on the jets dynamics is clear from the power spectra where the energy peak around ϕ is the second lowest of the eight studied cases, as can be seen in Table 2, and the lowest of the five cases with the applied frequency, $f = \phi$.

The cases promoting the highest dynamics of the jets oscillations are the ones with out-of-phase perturbations, mostly the ones with the highest amplitudes. At $A_l = A_r = 1.00$, as can be seen from the time histories, the jets oscillations are mainly determined from the imposed pulsation, while on the other cases there is a strong interaction between the flow field natural oscillations and imposed oscillations by pulsation. This result suggest that the flow field somehow preserves its own dynamics that emerges from the unsteady balance of the two opposite forces: the jets that have a velocity of 3.333m/s and are stopped by another jet in a distance of 5mm, up to pulsation values of 50% of the inlet flow rate. The cases where

$A_l = A_r = 0.50$, Cases 2, 3, 5, 7 and 8, all show periods where pulsation imposes over natural oscillation and vice versa, as can be seen on short periods of some time histories shown in Figure 3, where two different types of oscillation can be observed. For the cases of out-of-phase pulsation where *f=ϕ* three cases were tested, Case 4, 5, and 6, with 25%, 50% and 100% amplitude, respectively. The jets oscillation energy peak at ϕ is higher than from Case 1 with no pulsation, but presents a small evolution from 25% to 50% amplitude, as can be seen from the values in Table 2. On the other hand, the energy peak in the 50 to 100 Hz range, typical of the fully developed vortices, continuously increase with the pulsation frequency, presenting the highest value for 100% amplitude as can be seen from Figure 3. The imposed dynamics is only observed to dominate when pulsation reaches amplitudes of 100% of the inlet flow rate, with the energy peak at $f = \phi$ raising one order of magnitude in comparison to 25% and 50% amplitude pulsations, with a single oscillatory behaviour being identifiable from the time history of Case 6 in Figure 2. For Cases 4 to 6, streamline maps of Figure 2 show the earlier appearance of fully developed vortices, that for Case 6, where $A_l = A_r = 1.00$, the vortices are generated at the jets inlet region, which is the reason for the increase of the energy peaks in the range of 50 to 100Hz.

For the double frequency oscillations, where $f = 2\phi$, the natural flow oscillations and the imposed oscillations interact in a complex fashion cancelling the high energy peaks above 100 Hz. Previous works that engage mixing in steady flows from pulsation also observed that, after a certain frequency, pulsation loses its dominant role over the flow field dynamics. Zhongliang *et al.* (2002) used an external electrokinetic flow control in a Y-jets mixer to interleave two streams, but increasing continuously the modulation frequency, it was observed that instead of smaller layers of each stream, two segregated streams were obtained. Niu *et al.* (2006a) pulsed the flow along a microchannel from lateral ports (Niu et al. 2006b), and reported the amplitude versus frequency values generating fully chaotic flow regimes. From the work of Niu *et al.* (2006a) it is observed that, for a fixed pulsation amplitude, the flow regime becomes steady with increasing pulsation frequency. The pulsation amplitude and frequency have to be increased simultaneously to keep the flow regime fully chaotic. On the other hand, for a fixed pulsation frequency, increasing the amplitude was observed to increase the mixing and flow dynamics by Niu *et al.* (2006a). The increase on pulsation frequency is thus, turning the imposed perturbations to the system too fast to cause a clear impact, and then to have a dominant role on the flow dynamics, its energy, i.e. amplitude, also has to be increased.

The highest energy peak is obtained with a pulsation frequency of *ϕ/2*, where the pulsation frequencies are close to the frequencies of oscillation caused by the evolution of fully developed vortices and sets the whole system into resonance. From the streamlines in Figure 2, the earlier formation of the fully developed vortices at the impingement point occupying the entire mixing chamber width is clearly observed for Case 8. These fully developed vortices were previously reported as the main mixing structure in RIM (Santos *et al.*, 2005).

To assess the effect of pulsation on the downstream fully developed vortices, the power spectra of v_x for the eight defined cases was computed and it is shown for z=22 mm (P2) in Figure 5, and for z=33 mm (P3) in Figure 6. The fully developed vortices generate a frequency peak, ψ between 50 and 100 Hz, of which the maximum spectral energy values for P2 and P3 are presented in Table 3. The highest energy corresponds to the cases where vortices are better defined or more regularly generated.

Case 7, where the pulsation frequency is not in the same range of any natural oscillation of this system, i.e. it is not resonating with the system (Williamson and Govardhan, 2004) but imposing to it, presents the second lowest energy and along with Case 3 generate the streamline maps with more distorted vortices as can be seen from Figure 1. Case 3 and 7 present a drop on the spectral energy of the highest peak around ψ frequency in comparison with Case 1, which has no imposed jets pulsation.

Case 3, although the pulsation frequency was $f = \phi$, has the lowest energy peaks in the range of 50 to 100 Hz, due to the previously observed fact that the opposed jets forces are kept symmetrical and so the introduced disturbance is not imposing to the flow field but annihilating itself.

Table -3 Maximum energy levels between 50Hz and 100Hz frequency at 33mm and 22 mm down the mixing chamber axis

Case Number	Max Energy, m	
	Z=22 mm	**Z=33 mm**
1	0.285	0.351
2	0.254	0.448
3	0.126	0.238
4	0.192	0.208
5	0.412	0.720
6	0.979	0.941
7	0.204	0.238
8	1.98	0.654

For the one side pulsation, a clear difference on the spectral energy around ψ is not observed when compared to the one with no pulsation, Case 1 power spectra. The main difference is observed in the P2 power spectra of Figure 5, where the introduced perturbation frequency, 200 Hz, still causes a measurable effect, which almost completely fades at P3 in Figure 6.

The maximum energies were obtained for the cases where the pulsation was performed as out-of-phase, but only for amplitudes equal or greater than 50%, Cases 5, 6, 7 and 8. In Case 4, although the applied frequency was equal to the natural frequency of the system i.e., $f = \phi$, and the pulsation of the jets was performed as out-of-phase, the amplitude was only 25% and the imposed pulsation with this

Case 1

Case 2

Case 3

Case 4

Case 5

Case 6

Case 7

Case 8
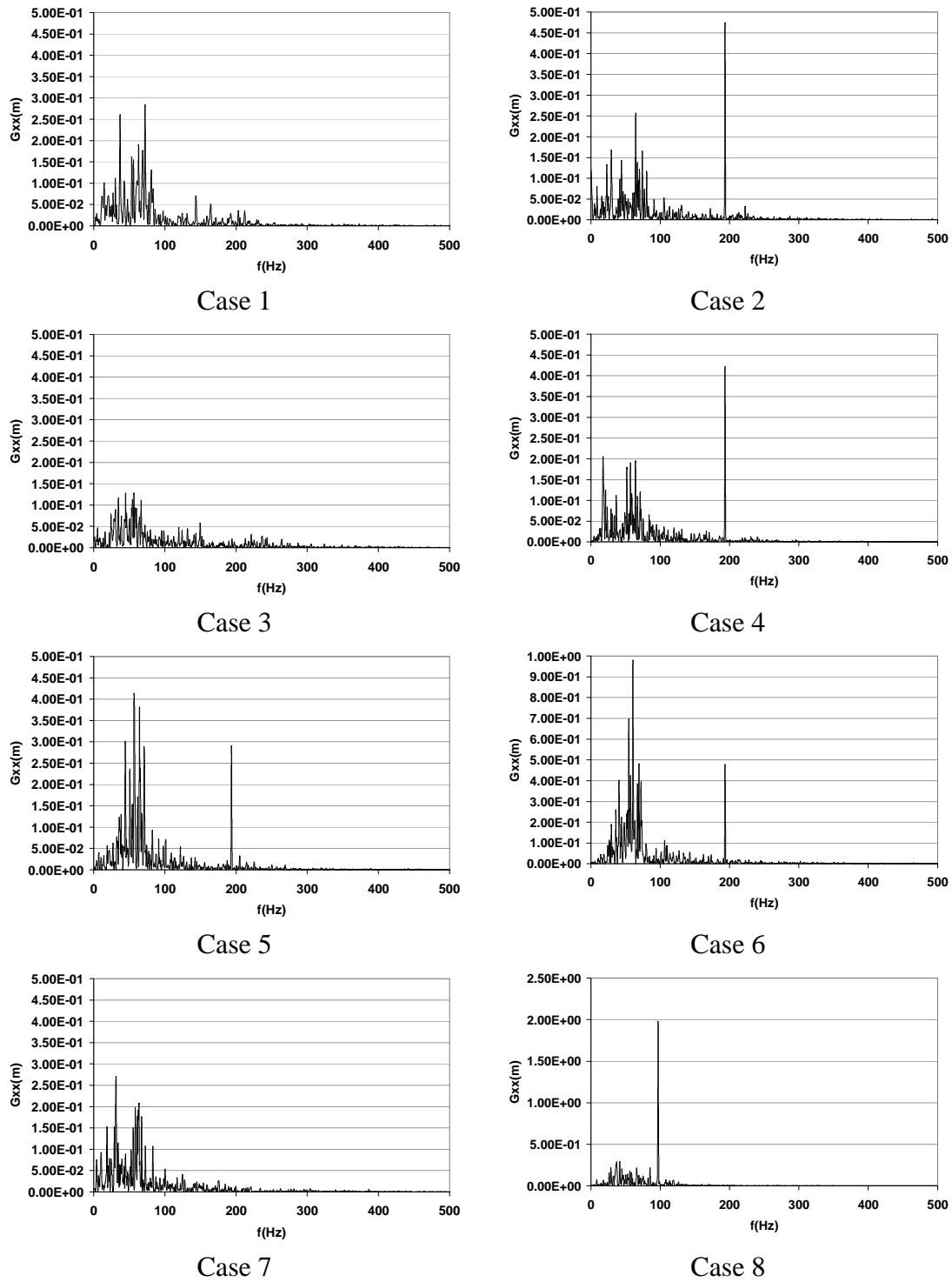
Figure 5 Power spectra at P2 from the dynamic simulations at average *Re*=300 using different pulsation strategies
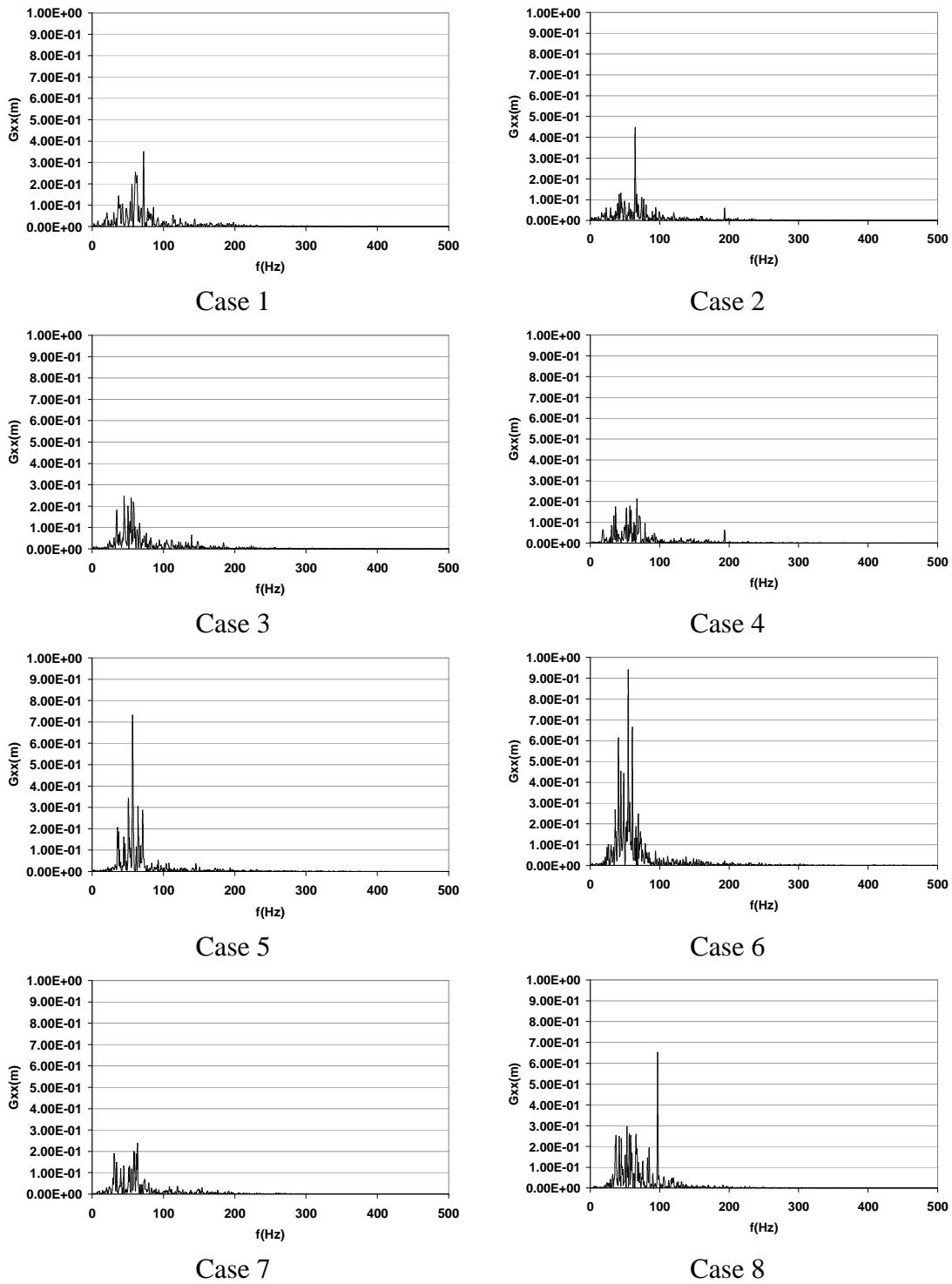
Figure 6 Power spectra at P3 from the dynamic simulations at average *Re*=300 using different pulsation strategies

amplitude did not create enough energy to impose the dynamics of the pulsation, instead, it causes a complex interaction with the natural flow dynamics of the system, and thus the spectral energy in the fully developed vortices range, 50 to 100Hz, is slightly lower than in the no pulsation Case 1. For Cases 5 and 6, where the amplitudes are 50% and 100%, respectively, an increase in the spectral energy around ψ, in comparison to Case 4, 25% amplitude pulsation, can be observed, and the energy peak value higher for the highest amplitude, Case 6, which has an energy level that is double of the one in Case 5. Thus, for higher pulsation amplitudes, the flow dynamics is mainly determined by the pulsation features, and the natural unforced flow dynamics is overridden.

For Case 8, where the pulsation frequency was closer to ψ, the spectral energy values caused by the fully developed vortices evolution at P2 were the highest, even though the imposed pulsation amplitude was not the maximum. It is then clear that pulsating the jets with frequencies near the fully developed vortices oscillation frequency can induce a more orderly flow of the vortex street. The value of f for Case 8 is not completely coincident with ψ, which is closer to 60 Hz. The pulsation frequency is thus imposing a new value of ψ but only up to P2, since on P3 the energy peak on 100 Hz frequency drops, and there is a raise of spectral energy around 60 Hz. It is then possible to impose a higher frequency of formation to the fully developed vortices in a short length before they evolve to their natural shape, i.e. the shape they would attain without pulsation. A higher frequency of the vortices is linked to smaller vortices, and consequently to a reduction on the scale of mixing.

Conclusions

In this article the enhancement of mixing through pulsation, namely its impact on the vortex formation and flow field dynamics inside the T-jets mixer RIM mixing chamber was studied
The frequency of pulsation was shown to have a clear impact on the flow dynamics:
- With values close to the natural jets oscillation frequencies, ϕ, pulsation enhances the regularity of the system which results in a clear oscillatory behaviour of the jets at the impingment point.
- With values close to the natural frequency of the fully developped vortices, ψ, pulsation can force the frequency of the fully develloped vortices passage and make it more orderly.

It was observed that the amplitude of the pulsation also has a strong effect on the flowfield:
- Lower amplitudes can not impose to the system dynamics resulting in an increase of flow randonness due to the interaction of two phenomena that cannot impose to each other, the own flow dynamics and the dynamic behaviour imposed from pulsation.
- Higher amplitudes, close to 100% of the flow rate, can completely dominate the dynamics of the flow field.

The other studied parameter was the impact of the pulsation strategy, which has shown that the strategies consisting of out-of-phase jets pulsation impose more clearly its dynamics to the system, since the displacement of the jets impingement point is completely determined from the pulsation. One side oscillation and on-phase oscillation were not able of imposing a clear influence on the flow field.

In the present work mass transfer is not actually assessed, as results only focused on the flow field and its dynamics. The interactions between pulsation and observed oscillations are too complex for any reasoning, and thus the quality of mixing will be assessed by coupling the chemical reaction to the simulations of these cases in future work.

This technology, registered as RIMCOP®, is part of a pending patent process (Lopes *et al.*, 2005) developed at LSRE/FEUP and now being commercialized by Fluidinova, Engenharia de Fluidos, SA.

References

Bierdel, M. and Piesche, M., *CFD - Simulation and Experimental Investigation of Impingement Mixing in Reaction Injection Molding (RIM)*, 3rd European Congress of Chemical Engineering, (2001).

Erkoç, E., Santos, R.J., Nunes, M.I., Dias, M.M., Lopes, J.C.B., *Mixing dynamics control in RIM machines*, Chemical Engineering Science, in press (2007).

Deshmukh, A.A., Liepmann, D. and Pisano, A., *Continuous micromixer with pulsatile micropumps*, Technical Digest of the IEEE Solid State Sensor and Actuator Workshop, 73-76 (2000).

Deshmukh, A.A., Liepmann, D. and Pisano, A., *Characterization of a micro-mixing, pumping, and valving system*, Proceedings of the 11th International Conference on Solid-State Sensors and Actuators, 779-782 (2001).

Ito, Y. and Komori, S., *A vibration technique for promoting liquid mixing and reaction in a microchannel*, AIChE Journal, 52, 3011-3017 (2006).

Johnson, D.A. and Wood, P.E., *Self-Sustained Oscillations in Opposed Impinging Jets in an Enclosure*, The Canadian Journal of Chemical Engineering, 78, 867-875 (2000).

Johnson, D.A., Wood, P.E. and Hrymak, A.N., *The Effect of Geometrical Parameters on the Flow Field of an Opposed Jet RIM Mix Head: Equal Flow and Matched Fluids.*, The Canadian Journal of Chemical Engineering, 74, 40-48 (1996).

Lopes, J.C.B., Santos, R.J., Teixeira, A.M. and Costa, M.R.P.F.N., *Production Process of Plastic Parts by Reaction Injection Moulding, and Related Head Device*, PCT, WO 2005/097477 (2005)

Lee, L.J., Ottino, J.M., Ranz, W.E. and Macosko, C.W., *Impingement Mixing in Reaction Injection Molding*, Polymer Engineering and Science, 20, 868-874 (1980).

Kolodziej, P., Macosko, C.W. and Ranz, W.E., *The Influence of Impingement Mixing on Striation Thickness Distribution and Properties in Fast Polyurethane Polymerization*, Polymer Engineering and Science, 22, 388-392 (1982).

Kolodziej, P., Yang, W.P., Macosko, C.W. and Wellinghoff, S.T., *Impingement Mixing and its Effect on the Microstructure of RIM Polyurethanes.*, Journal of Polymer Science, 24, 2359-2377 (1986).

Kusch, H.A., Ottino, J.M. and Shannon, D.M., *Analysis of Impingement Mixing-Reaction Data: Use of a Lamellar Model to Generate Fluid Mixing Information.*, Industrial & Engineering Chemistry Research, 28, 302-315 (1989).

Macosko, C.W., *RIM, Fundamentals of Reaction Injection Moulding*, Hanser ed.,Munich (1989).

Niu, X., Liu, L., Wen, W. and Sheng, P., *Hybrid Approach to High-Frequency Microfluidic Mixing*, Physical Review Letters, 97, 044501-4 (2006a).

Niu, X., Liu, L., Wen, W. and Sheng, P., Active microfluidic mixer chip, Applied Physics Letters, 88, 153508-3 (2006b).

Santos, R.J., Teixeira, A.M., Costa, M.R.P.F.N. and Lopes, J.C.B., *Operational and Design Study of RIM Machines*, International Polymer Processing, 17, 387-394 (2002).

Santos, R.J., Teixeira, A.M. and Lopes, J.C.B., *Study of Mixing and Chemical Reaction in RIM*, Chemical Engineering Science, 60, 2381-2398 (2005).

Teixeira, A.M., Santos, R.J., Costa, M.R.P.F.N. and Lopes, J.C.B., *Hydrodynamics of the Mixing Head in RIM: LDA Flow-Field Characterisation*, AIChE Journal, 51, 1608-1619 (2005).

Trautmann, P. and Piesche, M., *Experimental Investigation on the Mixing Behaviour of Impingement Mixers for Polyurethane Production*, Chemical Engineering and Technology, 24, 1193-1197 (2001).

Tucker, C.L. and Suh, N.P., *Mixing for Reaction Injection Molding. I. Impingement Mixing of Liquids.*, Polymer Engineering and Science, 20, 875-886 (1980).

Williamson, C.H.K. and Govardhan, R., *Vortex-induced vibrations*, Annual Reviews of Fluid Mechanics, 36, 413-455 (2004).

Wood, P., Hrymak, A.N., Yeo, R., Johnson, D.A. and Tyagi, A., *Experimental and Computational Studies of the Fluid Mechanics in an Opposed Jet Mixing Head*, Phys. Fluids A, 3, 1362-1368 (1991).

Xiaojin, L., Santos, R., Lopes, J.C., *Modeling of Self-Induced Oscillations in the Mixing Head of a RIM Machine*, The Canadian Journal of Chemical Engineering, 85, 45-54 (2007).

Zhongliang, T., Seungbae, H., Djordje, D., Vijay, M., Alan, C.W., James, Y. and Richard, M.O., *Electrokinetic flow control for composition modulation in a microchannel*, Journal of Micromechanics and Microengineering, 12, 870 (2002).